



Toward Models for the Full Oxygen-Evolving Complex of Photosystem II by Ligand Coordination To Lower the Symmetry of the Mn_3CaO_4 Cubane: Demonstration That Electronic Effects Facilitate Binding of a Fifth Metal

Jacob S. Kanady, Po-Heng Lin, Kurtis M. Carsch, Robert J. Nielsen, Michael K. Takase, William A. Goddard, III, and Theodor Agapie*

Division of Chemistry and Chemical Engineering, California Institute of Technology, Pasadena, California 91125, United States

S Supporting Information

ABSTRACT: Synthetic model compounds have been targeted to benchmark and better understand the electronic structure, geometry, spectroscopy, and reactivity of the oxygen-evolving complex (OEC) of photosystem II, a low-symmetry Mn_4CaO_n cluster. Herein, low-symmetry $\text{Mn}^{\text{IV}}_3\text{GdO}_4$ and $\text{Mn}^{\text{IV}}_3\text{CaO}_4$ cubanes are synthesized in a rational, stepwise fashion through desymmetrization by ligand substitution, causing significant cubane distortions. As a result of increased electron richness and desymmetrization, a specific μ_3 -oxo moiety of the Mn_3CaO_4 unit becomes more basic allowing for selective protonation. Coordination of a fifth metal ion, Ag^+ , to the same site gives a $\text{Mn}_3\text{CaAgO}_4$ cluster that models the topology of the OEC by displaying both a cubane motif and a “dangler” transition metal. The present synthetic strategy provides a rational roadmap for accessing more accurate models of the biological catalyst.

The oxygen-evolving complex (OEC) of photosystem II (PSII) is the sole biological water oxidation catalyst.¹ During the catalytic cycle, the OEC is photo-oxidized four times, affording the high-oxidation-state Mn necessary for O–O bond formation and release of O_2 .¹ The structure of this heterometallic Mn/Ca cluster has been investigated through spectroscopic,² X-ray diffraction (XRD),³ and computational⁴ studies that support a low-symmetry Mn_4CaO_n cluster containing a distorted Mn_3CaO_4 cubane bridged to a fourth manganese through one oxygen of the cubane and a μ_2 -oxo. The redox-inactive Ca^{2+} has been shown experimentally to be crucial for catalytic activity,⁵ and multiple computational studies include the fourth, dangling Mn as an integral part of the catalytic cycle.^{4,6}

Recently, the Mn_3CaO_4 cubane subsite of the OEC has been accurately modeled,⁷ providing electrochemical details suggesting that Ca^{2+} plays a role in tuning the reduction potentials of the Mn centers.^{7a,8} Based on EPR and magnetism measurements, cluster asymmetry, or distortion, in the Mn_3CaO_4 unit, manifested in one case by coordination of a cubane oxo to a second Ca^{2+} , was proposed to affect the cluster electronic structure and thus its chemical reactivity.^{7b} Low-symmetry, heterometallic Mn_3MO_4 cubane complexes are therefore

desirable synthetic targets for further electronic structure studies and as precursors to full Mn_4CaO_n models of the OEC.

We have developed synthetic protocols to facilitate rational design of site-differentiated, homo- and heterometallic metal-oxo clusters.^{7a,8,9} The 1,3,5-triphenylbenzene-based ligand scaffold (**L**, Scheme 1) results in Mn_3MO_4 cubanes that have high, *pseudo*- C_3 symmetry and an apical metal, M, labile to substitution by more Lewis acidic ions.⁸ For example, Mn_3CaO_4 cubane complex **1** reacts quantitatively with $\text{Mn}^{\text{II}}(\text{OTf})_2 \cdot 2\text{CH}_3\text{CN}$ (OTf = trifluoromethanesulfonate) to yield the reported Mn_4O_4 cubane **2** rapidly upon mixing (Scheme 1). This substitution prohibits appending a fourth Mn to **1** to generate a model of the full OEC. Herein, we report strategies to distort and stabilize Mn_3MO_4 cubanes, forming a pentametallic complex in the biologically relevant geometry as a first example of the $\text{Mn}_3\text{CaM}'\text{O}_4$ unit with a dangling transition metal.

The Mn_3MO_4 cubanes supported by ligand **L** display alkoxide and pyridine coordination to the three Mn_2O_2 faces (“bottom” of the cubane) and acetate bridging the three MnMO_2 faces (“top” of the cubane). Solvent molecules complete the coordination sphere of larger cations M (Scheme 1, complexes **1–3**), such as Ca^{2+} , Sc^{3+} , Y^{3+} , and Ln^{3+} , with coordination numbers up to nine being observed.^{7a,8,9e} Substitution of the solvent molecules and acetates with multidentate ligands offers the opportunity to rationally modify the structure and properties of the cubane. We selected the design elements of this multidentate ligand to address several aspects: (1) lower the propensity for substitution for the top metal, M, by a fifth metal equivalent, M'; (2) distort the cubane; and (3) change the reactivity of the cubane unit to allow incorporation of a fifth metal, M'. The $\text{Mn}^{\text{IV}}_3\text{GdO}_4$ cubane **3** was chosen for initial studies since the size of Gd^{3+} affords more coordination sites and Gd^{3+} is less susceptible to metal substitution. The substitution of the acetates of $\text{Mn}^{\text{IV}}_3\text{MO}_4$ cubanes is significantly slower than for cubanes displaying Mn^{III} centers, as demonstrated by isotopic scrambling experiments with acetate- d_3 and acetate- d_0 .^{9b} Therefore, multidentate ligands were chosen that could bind not only to the top metal (Gd^{3+} or Ca^{2+}) but also to at least one

Received: August 8, 2014

Published: September 20, 2014



LMn^{IV}₃CaO₄(OAc)₃(THF) (1)

Mn(OTf)₂ (1.0 equiv)
DMF, 20 min, >95%

Gd(OTf)₃ (1.0 equiv)
DMF, 1 hr, quant.

"HON₄OH" (1 equiv)
NEt₃ (2 equiv)
THF, r.t., 12 hr, 91%

AgOTf (1.8 equiv)
20:1 DCM/ACN
12 hr

*Complex rotated by ca. 120°

LutHOTf (1.05 equiv)
DCM, 2 hr, quant.

Oxygen-Evolving Complex

Ala₃₄₄, Asp₃₄₂, Glu₁₈₉, Asp₁₇₀, Glu₃₅₄, His₃₃₂, Glu₃₃₃

favorable five-membered rings. The binding of $[\text{ON}_4\text{O}]^{2-}$ generates a low-symmetry cubane core compared to **3**. The structural parameters (Figure 2) show that the μ_3 -oxo moieties of **3** have more uniform Mn–O bond lengths (1.841(2)–1.916(2) Å), than in **4** (1.844(5)–1.946(4) Å), with the bonds trans to the oximate ligands elongated due to the higher trans influence of these donors compared to acetates. Additionally, the Gd–O2 distance is shortened, likely due to a combination of increased basicity at O2, increased acidity at Gd, and the chelating effect of the $[\text{ON}_4\text{O}]^{2-}$. The ^1H NMR spectrum of **4** shows an increased number of peaks relative to **3** and the electrospray ionization mass spectrometry (ESI-MS) masses support bound $[\text{ON}_4\text{O}]^{2-}$ and loss of two acetates, both

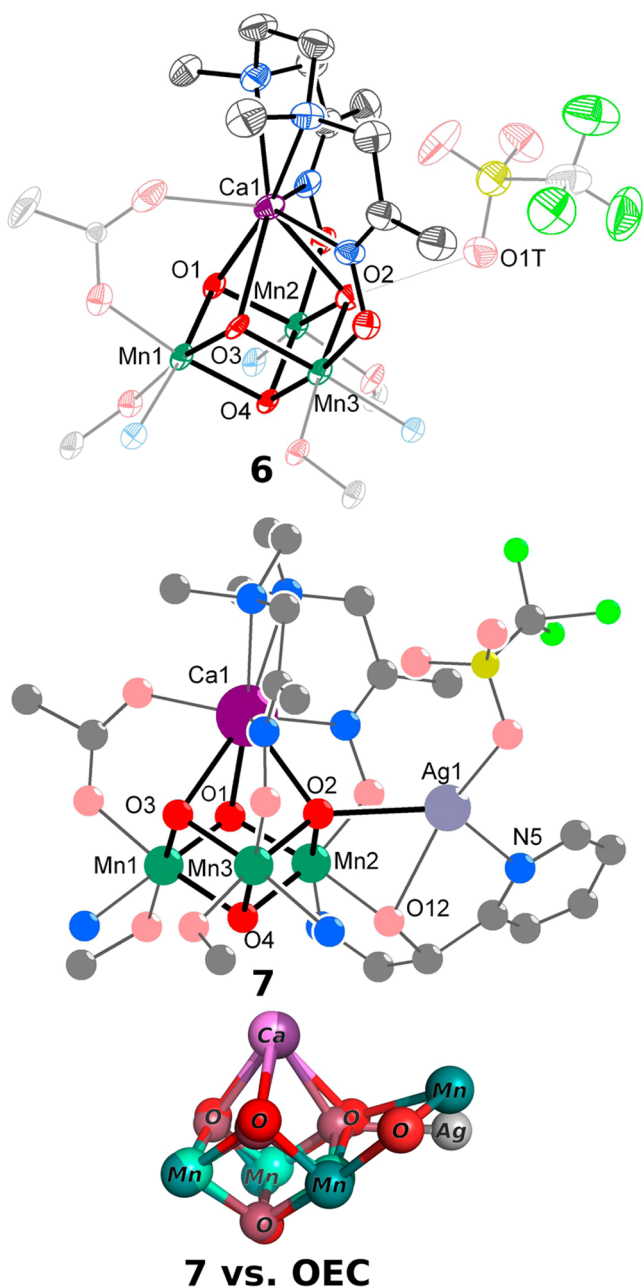


Figure 3. Truncated solid-state structure of **6** and **7**, with the core of **7** and the OEC overlaid.^{3b} Hydrogens and outer-sphere anions not shown for clarity.

consistent with the low symmetry observed in the solid state persisting in solution.

With the Mn_3GdO_4 system as a proof-of-principle that low-symmetry cubane structures could be built on ligand scaffold **1**, the Mn_3CaO_4 system was targeted next as a more accurate model of the OEC. Addition of HON_4OH to **1** in DMF followed by heating to 80 °C precipitated complex **5** after 45–60 min. Complex **5** has low solubility in all solvents tested, which has precluded the generation of X-ray-quality single crystals for structural determination, but ESI-MS shows one main peak at m/z 1412, consistent with the proposed structure where two acetates have been substituted by the $[\text{ON}_4\text{O}]^{2-}$ moiety as in **4**. Addition of acid, 2,6-lutidinium triflate (LutHOTf), to **5** gave new paramagnetic signals and disappearance of the acidic proton of $[\text{LutH}]^+$ at 15 ppm in

the ^1H NMR spectrum, a similar mass to **5** by ESI-MS, and increased solubility. Indeed, an XRD study of the resulting complex **6** reveals that ON_4O has substituted two acetates as observed for **4**, implying that the oximate had been bound to precursor **5**. The Ca^{2+} center is 8-coordinate, higher than in precursor **1**. Analysis of the structural parameters of the MnCaO_4 core reveals that it is asymmetric. In particular, an outer sphere triflate anion is found in close proximity ($\text{O1T}-\text{O2} = 2.660(8)$ Å) to the $\mu_3\text{-O}$ moiety that coordinates to Ca^{2+} and to the Mn centers supported by the oximates. This distance suggests protonation at this position to generate a $\mu_3\text{-OH}$ moiety involved in a hydrogen bonding interaction with the triflate.¹⁰ In agreement, the Mn–O2 distances (1.926(5), 1.944(5) Å) of **6** are longer than in **1**, **4** and the other top oxo O–Mn distances in **6** by 0.05–0.1 Å (Figure 2). Compound **6** is the first structurally characterized example of a protonated high oxidation state Ca–Mn mixed oxide cluster. The significant distortion promoted by protonation correlates to studies of the OEC.¹¹

The symmetric Mn_3CaO_4 cubane **1** does not react with LutHOTf in DCM (Supporting Information (SI), Figure S9). Therefore, the protonation of the $\text{Mn}^{\text{IV}}_3\text{CaO}_4$ core specifically at O2 suggests that the $[\text{ON}_4\text{O}]^{2-}$ ligand promotes (1) an increase in the electron richness of the cluster, as oximates are more basic than carboxylates, and (2) electronic desymmetrization of the cluster, together making the O2 site significantly more basic. This effect was further studied by quantum mechanics (B3LYP-D3 DFT, see SI) through the inspection of both canonical (nonlocal) and localized molecular orbitals. Ground-state optimizations of simplified models for **1** (**1m**), **5** (**5m**), and **6** (**6m**) were performed, showing good agreement with the crystal structures (RMS values of 0.024 Å (**1**) and 0.037 Å (**6**)). Analysis of localized molecular orbitals shows that the energy of O2 changes the most during ligation of $[\text{ON}_4\text{O}]^{2-}$. The energies of the three equatorial $\mu_3\text{-oxo}$ motifs of **1m** appear effectively degenerate (−0.72, −0.71, and −0.72 hartrees). Upon coordination of $[\text{ON}_4\text{O}]^{2-}$, the energies of the oxides' localized lone pairs are all higher in energy, consistent with a more electron rich cluster as expected for oximate vs acetate coordination. Notably, lowering the symmetry of the cubane (**5m**) leads to different lone pair energies for O2, O1, and O3 (−0.56, −0.69, and −0.66 hartrees), with the largest change occurring for O2. This asymmetry is reflected experimentally in the protonation of **5** at the O2 position to generate **6**. Upon protonation of the most basic $\mu_3\text{-oxo}$, the $\mu_3\text{-hydroxo}$ and the two $\mu_3\text{-oxo}$ moieties shift energy to −0.61 ($\sigma_{\text{O}^*\text{-H}}$ bond), −0.70, and −0.70 hartrees (lone pairs), respectively, in **6m**. The canonical molecular orbitals reflect the notions above (SI, Figures S11–S13) by showing higher energy for the HOMO of **5m** vs **1m** and increase in electron density at the O2 position.

With the increased Lewis basicity of $\mu_3\text{-oxo}$ O2 established, binding of a “dangler” metal instead of a proton at this position was targeted to model the $\text{Mn}_3\text{CaO}_4 + \text{M}'$ geometry of the OEC.¹² Addition of metal triflate salts of Ag^+ , Mn^{2+} , and Co^{2+} to **5** led to changes in the ^1H NMR and ESI-MS spectra, indicative of productive reactions (see SI). None showed loss of Ca^{2+} as compared to **1**, a crucial finding for further cluster elaboration. Moreover, the ESI-MS spectra of the Mn and Co reactions displayed peaks consistent with $\text{LMn}_3\text{CaO}_4(\text{ON}_4\text{O})\text{-(OAc)·M'-(OTf)}$ and $\text{LMn}_3\text{CaO}_4(\text{ON}_4\text{O})(\text{OAc})\text{·M'-(H}_2\text{O)}_2$, with fragmentation patterns corresponding to loss of OTf^- and H_2O , respectively, suggesting the formation of the desired

Mn₃CaM' stoichiometry in solution (SI, Figures S10–S15). Crystals suitable for XRD studies were obtained only from the reaction of **5** with AgOTf to generate cluster **7** (Figure 3). The quality of the XRD data is low, but does allow confirmation of connectivity. The solid-state structure of product **7** shows a Mn₃CaAgO₄ cluster. Due to the quality of the data the identity of the silver atom is not certain; however, the chemical coordination, bond distances, and displacement parameters are more consistent with Ag than Mn or Ca. The “dangling” Ag⁺ is directly linked to the cubane core via coordination to a μ_4 -oxo, one μ_2 -alkoxide, and one of the pyridines of **L** that was not coordinated in the precursors. The fourth coordination site is filled by a triflate. Ca²⁺ is in a similar geometry to **6**. An overlay of the structures of the OEC and **7** shows that the geometry of the Mn₃CaM'O₄ clusters is well modeled (Figure 3). This represents the first example of rational, stepwise synthesis of the asymmetric pentametallic core model of the OEC. Starting from a trimanganese precursor, addition of Ca²⁺ and oxidation lead to the cubane core,^{7a} which is then desymmetrized and further elaborated with addition of the “dangler” metal. Conceptually related, the photoassembly of the OEC also involves several intermediates with stepwise incorporation of metals, although in a different order than demonstrated synthetically here.^{13,14} Additionally, the tuning of the basicity of coordinated OH_x moieties by metal ions has been invoked in the assembly of the biological cluster.¹⁵

In summary, starting from *pseudo*-C₃ symmetric Mn^{IV}₃CaO₄ and Mn^{IV}₃GdO₄ cubanes, coordination of a multidentate bisoximate ligand leads to lower-symmetry clusters. Most notably, the oximate ligand stabilizes the Mn^{IV}₃CaO₄ core against Ca²⁺ substitution. The cluster is affected electronically to increase the basicity of one of the oxo moieties, which can be selectively protonated to generate a Mn^{IV}₃CaO₃(OH) cluster. The basicity of this site can also be exploited to coordinate a fifth metal. A Mn^{IV}₃CaAgO₄ cluster was structurally characterized, showing high structural similarity to the OEC. The present compounds provide insight into the electronic tunability of clusters related to the OEC by ligand binding. Additionally, the reported strategy provides the first rational synthetic roadmap for accessing more accurate models of the biological catalyst.

■ ASSOCIATED CONTENT

■ Supporting Information

Synthetic procedures, spectroscopic characterization, crystallographic data, and computational details and results. This material is available free of charge via the Internet at <http://pubs.acs.org>.

■ AUTHOR INFORMATION

Corresponding Author

agapie@caltech.edu

Notes

The authors declare no competing financial interest.

■ ACKNOWLEDGMENTS

This work was supported by the California Institute of Technology, the NIH (R01 GM102687A, T.A.), the NSF GRFP (J.S.K.), and NSF (CHE-1214158, W.A.G.). T.A. is a Sloan, Dreyfus, and Cottrell fellow. We thank Lawrence M. Henling for assistance with crystallography. The Bruker KAPPA APEXII X-ray diffractometer was purchased via an NSF

Chemistry Research Instrumentation award to Caltech (CHE-0639094).

■ REFERENCES

- (1) (a) Wydrzynski, T.; Satoh, K. *The Light-Driven Water: Plastiquinone Oxidoreductase*; Springer: Dordrecht, 2005; Vol. 22. (b) McEvoy, J. P.; Brudvig, G. W. *Chem. Rev.* **2006**, *106*, 4455. (c) Yano, J.; Yachandra, V. *Chem. Rev.* **2014**, *114*, 4175.
- (2) (a) Peloquin, J. M.; Campbell, K. A.; Randall, D. W.; Evanchik, M. A.; Pecoraro, V. L.; Armstrong, W. H.; Britt, R. D. *J. Am. Chem. Soc.* **2000**, *122*, 10926. (b) Yano, J.; Kern, J.; Sauer, K.; Latimer, M. J.; Pushkar, Y.; Biesiadka, J.; Loll, B.; Saenger, W.; Messinger, J.; Zouni, A.; Yachandra, V. K. *Science* **2006**, *314*, 821. (c) Pantazis, D. A.; Ames, W.; Cox, N.; Lubitz, W.; Neese, F. *Angew. Chem., Int. Ed.* **2012**, *51*, 9935.
- (3) (a) Ferreira, K. N.; Iverson, T. M.; Maghlaoui, K.; Barber, J.; Iwata, S. *Science* **2004**, *303*, 1831. (b) Umena, Y.; Kawakami, K.; Shen, J.-R.; Kamiya, N. *Nature* **2011**, *473*, 55.
- (4) (a) Siegbahn, P. E. M. *Chem.—Eur. J.* **2006**, *12*, 9217. (b) Sproviero, E. M.; Gascón, J. A.; McEvoy, J. P.; Brudvig, G. W.; Batista, V. S. *J. Am. Chem. Soc.* **2008**, *130*, 3428. (c) Siegbahn, P. E. M. *Chem.—Eur. J.* **2008**, *14*, 8290. (d) Ames, W.; Pantazis, D. A.; Krewald, V.; Cox, N.; Messinger, J.; Lubitz, W.; Neese, F. *J. Am. Chem. Soc.* **2011**, *133*, 19743. (e) Siegbahn, P. E. *Biochim. Biophys. Acta* **2013**, *1827*, 1003.
- (5) (a) Sivaraja, M.; Tso, J.; Dismukes, G. C. *Biochemistry* **1989**, *28*, 9459. (b) Yocum, C. F. *Coord. Chem. Rev.* **2008**, *252*, 296.
- (6) Siegbahn, P. E. M. *J. Am. Chem. Soc.* **2013**, *135*, 9442.
- (7) (a) Kanady, J. S.; Tsui, E. Y.; Day, M. W.; Agapie, T. *Science* **2011**, *333*, 733. (b) Mukherjee, S.; Stull, J. A.; Yano, J.; Stamatatos, T. C.; Pringouri, K.; Stich, T. A.; Abboud, K. A.; Britt, R. D.; Yachandra, V. K.; Christou, G. *Proc. Natl. Acad. Sci. U.S.A.* **2012**, *109*, 2257.
- (8) Tsui, E. Y.; Agapie, T. *Proc. Natl. Acad. Sci. U.S.A.* **2013**, *110*, 10084.
- (9) (a) Tsui, E. Y.; Tran, R.; Yano, J.; Agapie, T. *Nat. Chem.* **2013**, *5*, 293. (b) Kanady, J. S.; Mendoza-Cortes, J. L.; Tsui, E. Y.; Nielsen, R. J.; Goddard, W. A., III; Agapie, T. *J. Am. Chem. Soc.* **2013**, *135*, 1073. (c) Kanady, J. S.; Tran, R.; Stull, J. A.; Lu, L.; Stich, T. A.; Day, M. W.; Yano, J.; Britt, R. D.; Agapie, T. *Chem. Sci.* **2013**, *4*, 3986. (d) Herbert, D. E.; Lionetti, D.; Rittle, J.; Agapie, T. *J. Am. Chem. Soc.* **2013**, *135*, 19075. (e) Lin, P.-H.; Takase, M. K.; Agapie, T. *Inorg. Chem.* **2014**, submitted.
- (10) (a) Aromí, G.; Wemple, M. W.; Aubin, S. J.; Folting, K.; Hendrickson, D. N.; Christou, G. *J. Am. Chem. Soc.* **1998**, *120*, 5850. (b) Papatriantafyllopoulou, C.; Abboud, K. A.; Christou, G. *Inorg. Chem.* **2011**, *50*, 8959. (c) Langley, S. K.; Chilton, N. F.; Moubaraki, B.; Murray, K. S. *Dalton Trans.* **2012**, *41*, 1033.
- (11) Glatzel, P.; Schroeder, H.; Pushkar, Y.; Boron, T.; Mukherjee, S.; Christou, G.; Pecoraro, V. L.; Messinger, J.; Yachandra, V. K.; Bergmann, U.; Yano, J. *Inorg. Chem.* **2013**, *52*, 5642.
- (12) The basicity and coordinating ability of the μ_3 -O moieties of a Co₄O₄ cubane have been evaluated: Dimitrou, K.; Folting, K.; Streib, W. E.; Christou, G. *J. Chem. Soc., Chem. Commun.* **1994**, *1994*, 1385.
- (13) The first Mn center to bind to the protein is coordinated by Asp170, a ligand that supports the dangler in the assembled OEC: Campbell, K. A.; Force, D. A.; Nixon, P. J.; Dole, F.; Diner, B. A.; Britt, R. D. *J. Am. Chem. Soc.* **2000**, *122*, 3754.
- (14) Dasgupta, J.; Ananyev, G. M.; Dismukes, G. C. *Coord. Chem. Rev.* **2008**, *252*, 347.
- (15) Tyrshkin, A. M.; Watt, R. K.; Baranov, S. V.; Dasgupta, J.; Hendrich, M. P.; Dismukes, G. C. *Biochemistry* **2006**, *45*, 12876.